



Universiteit
Leiden
The Netherlands

Transport dynamics and physiological responses of polystyrene nanoplastics in pakchoi: implications for food safety and environmental health

Liu, Z.; Qin, M.; Li, R.; Peijnenburg, W.J.G.M.; Yang, L.; Liu, P.; Shi, Q.

Citation

Liu, Z., Qin, M., Li, R., Peijnenburg, W. J. G. M., Yang, L., Liu, P., & Shi, Q. (2025). Transport dynamics and physiological responses of polystyrene nanoplastics in pakchoi: implications for food safety and environmental health. *Journal Of Agricultural And Food Chemistry*, 73(18), 10923-10933. doi:10.1021/acs.jafc.5c03590

Version: Publisher's Version

License: [Licensed under Article 25fa Copyright Act/Law \(Amendment Taverne\)](#)

Downloaded from: <https://hdl.handle.net/1887/4246610>

Note: To cite this publication please use the final published version (if applicable).

Transport Dynamics and Physiological Responses of Polystyrene Nanoplastics in Pakchoi: Implications for Food Safety and Environmental Health

Zhiguo Liu, Mengzhan Qin, Runze Li, Willie J.G.M. Peijnenburg, Long Yang, Peng Liu,* and Qinghua Shi



Cite This: *J. Agric. Food Chem.* 2025, 73, 10923–10933



Read Online

ACCESS |



Metrics & More



Article Recommendations



Supporting Information

ABSTRACT: Nanoplastics (NPs) have become a new environmental pollutant that causes serious harm to food safety. They can be absorbed by plants, transported to edible parts, transmitted to the human body along the food chain, and can threaten human health. The research investigated the transport and accumulation pathways of polystyrene NPs (PS-NPs) at varying concentrations using red fluorescence labeling. An analysis was conducted on the response of pakchoi to PS-NPs through a combination of transcriptional and physiological experiments. PS-NPs enter the xylem vessel of the root, subsequently carried to the petiole through transpirational tension, and eventually transported from the petiole's xylem vessels to the leaf. PS-NPs induced the accumulation of reactive oxygen species (ROS), which led to oxidative damage. In addition, it also disturbed the homeostasis of endogenous hormones and affected the growth of pakchoi. These findings help people understand the adverse effects of NPs on crops and increase attention to the hazards of NPs.

KEYWORDS: *Pakchoi, nanoplastics, phytotoxicity, oxidative stress, hormone homeostasis*

1. INTRODUCTION

Plastics are widely used across various sectors, including industry, agriculture, and everyday activities, due to their cost-effectiveness, lightweight nature, flexibility, and resilience.¹ Global microplastic (MP) emissions currently range between 10 and 40 million metric tons annually, with projections suggesting a potential doubling under business-as-usual scenarios by 2040.² The International Agency for Research on Cancer (IARC) has classified various types of plastics, derivatives, and components, including polyvinyl chloride (PVC) derivatives, PS, and phthalates, as potentially carcinogenic.³ Despite the growing awareness of the detrimental effects of plastic on the global environment, the production of plastic continues to rise at an alarming rate. Projections indicate that plastic production could reach an astounding 34 billion tons by 2050.⁴ Although plastic recycling and management policies continue to improve, it is reported that only 9% of plastic waste is recycled, 12% is incinerated, and the remaining 79% is landfilled.^{2,5}

According to the research of Wang et al., samples from six land-use types were collected from Chinese farmlands in five provinces.⁶ It was found that MP abundances were in the range of 2783–6366 items/kg in all samples. In regions characterized by severe plastic pollution, the concentration of plastics in the soil can reach levels ranging from 300 to 67,500 mg kg⁻¹.⁷ Plastics in the soil gradually degrade into MPs and NPs through various processes, including ultraviolet radiation, thermal oxidation, mechanical wear, and biodegradation.⁸ Among them, those with sizes between 100 nm and 5 mm are called MPs, including submicron (100 nm to 1 μm) and

micron (1 μm to 5 mm) plastics, while those with sizes between 1 and 100 nm are called NPs.⁹ Li et al. categorized MPs into five size ranges: <0.2, 0.2–0.5, 0.5–1, 1–2, and 2–5 mm.¹⁰ Their findings indicated that across soil layers of varying depths in different plots, the proportion of MPs smaller than 0.2 mm was consistently the highest. Notably, in the 40–60 cm soil layer of the grassland, this proportion reached 89.7%. NPs are likely more hazardous to living organisms than MPs due to their greater abundance and reactivity. NPs disperse more rapidly in the environment, can infiltrate living cells, and exhibit higher accumulation within organisms compared to MPs.^{11–13} Consequently, NPs warrant more focused research and attention than MPs.

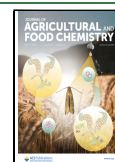
Bandmann et al. demonstrated that when the size of nanobeads is sufficiently small (≤40 nm), they can penetrate tobacco cells via endocytosis.¹⁴ In contrast, nanobeads measuring 100 nm are obstructed by the cell wall and are unable to enter the cells through this mechanism. Larger-sized NPs enter the root system through cracks formed at the lateral root buds of plants and are subsequently transported from the roots to the shoots, driven by transpiration tension.⁹ NPs inflict multiple harms on plants, including, but not limited to, accumulation in chloroplasts, which leads to the degradation of

Received: March 23, 2025

Revised: April 16, 2025

Accepted: April 17, 2025

Published: April 29, 2025



thylakoids and inhibits photosynthesis.^{15,16} Additionally, they induce the accumulation of ROS, resulting in oxidative damage.^{17,18} NPs obstruct the pores of the cell wall, inhibiting the absorption and transport of nutrients^{19,20} and disrupting the homeostasis of plant endogenous hormones.^{21,22} Ultimately, these effects culminate in stunted plant growth and a reduction in both yield and quality.^{23,24}

PS is one of the most common MPs and is mainly used in producing CDs, toys, toothbrushes, foam products, etc.²⁵ Previous studies have demonstrated that PS-NPs exhibit significant toxicity to microorganisms, plankton, invertebrates, and vertebrates.^{26–30} In addition, plants exposed to PS-NPs will also produce adverse symptoms such as growth inhibition, increased reactive oxygen species, reduced photosynthetic rate, and disordered transcription and metabolic processes, which have been reported in *Arabidopsis thaliana*, wheat, corn, rice, barley, soybean, peanut, cotton, lettuce, spinach, Chinese cabbage, tomato, cucumber, onion, and strawberry.^{31–45}

Conti et al. detected the presence of MPs in daily consumed fruits and vegetables, which raised further concerns about food safety.⁴⁶ Pakchoi (*Brassica rapa* L. subsp. *Chinensis*) is rich in vitamins and minerals and is an important vegetable crop in Asia.⁴⁷ Although studies have demonstrated that the presence of MPs adversely affects the growth of pakchoi,^{48,49} the absence of NPs treatment precludes the provision of direct evidence regarding the accumulation of NPs within the pakchoi's tissues. In this study, pakchoi seedlings were treated with 50 nm PSs labeled with varying concentrations of red fluorescence. The transport mechanism of NPs in pakchoi was elucidated using confocal laser scanning microscopy (CLSM) and scanning electron microscopy (SEM). Additionally, the molecular and physiological mechanisms underlying NP-induced toxicity in pakchoi were analyzed through transcriptomic and physiological experiments. These results clearly indicate that NPs can accumulate in vegetable crops, leading to reduced yields and posing potential risks to food safety and human health. Therefore, to ensure the sustainable development of agriculture, it is imperative that we acknowledge the risks associated with NP pollution and promptly implement relevant policies to minimize the use and emissions of plastics.

2. MATERIALS AND METHODS

2.1. PS-NP Solution Characterization. The spherical PS-NPs were purchased from Huge Biotechnology (Shanghai, China). PS-NPs have a particle size of 50 nm, red fluorescence, and excitation wavelength and emission wavelength are 535 and 610 nm, respectively. The primary concentration of PS-NPs was 25 mg mL⁻¹, which was subsequently diluted to concentrations of 25, 50, and 100 mg L⁻¹ using deionized water, followed by sonication for 30 min. Transmission electron microscopy (TEM) observation found that the shape of PS-NPs was spherical, and the size was about 50 nm (Figure S1A). The particle size distribution of PS-NPs is shown in Figure S1B.

2.2. Plant Material and Treatment. The pakchoi variety used in this experiment is "Jinzi 30". Pakchoi seeds were sown in the planting sponge and put into a light incubator (Thermo Scientific, 3943TS); temperature was 26 °C, humidity was 65%, light intensity was 300 μmol m⁻² s⁻¹, 16 h of light, and 8 h of darkness growth for 7 days. The pakchoi seedlings with consistent growth were selected and moved into the black hydroponic box filled with 2 L of 1/2 Hoagland solution (Coolaber, NS1011). Each hydroponic box contained four pakchoi seedlings and continued to grow for 7 days. Different concentrations of PS-NPs were used for the following treatments: CK: 1/2 Hoagland without PS-NPs, NP10: 1/2 Hoagland with 10 mg L⁻¹ PS-NPs, NP50: 1/2 Hoagland with 50 mg L⁻¹ PS-NPs, and

NP100: 1/2 Hoagland with 100 mg L⁻¹ PS-NPs; for the setting of PS-NPs concentration, refer to Sun et al., which was much lower than the number of plastics in heavily polluted areas.¹⁷ Hence, the NP concentration we used was reasonable. Five replicates were taken per treatment, and samples were taken 2 weeks after treatment.

2.3. Biomass Determination. A pakchoi seedling from each treatment was randomly selected, placed on a black curtain, used a 5 cm white label as a ruler, and pictures taken with a camera (Figure 1A). The pakchoi seedlings with different treatments were rinsed with

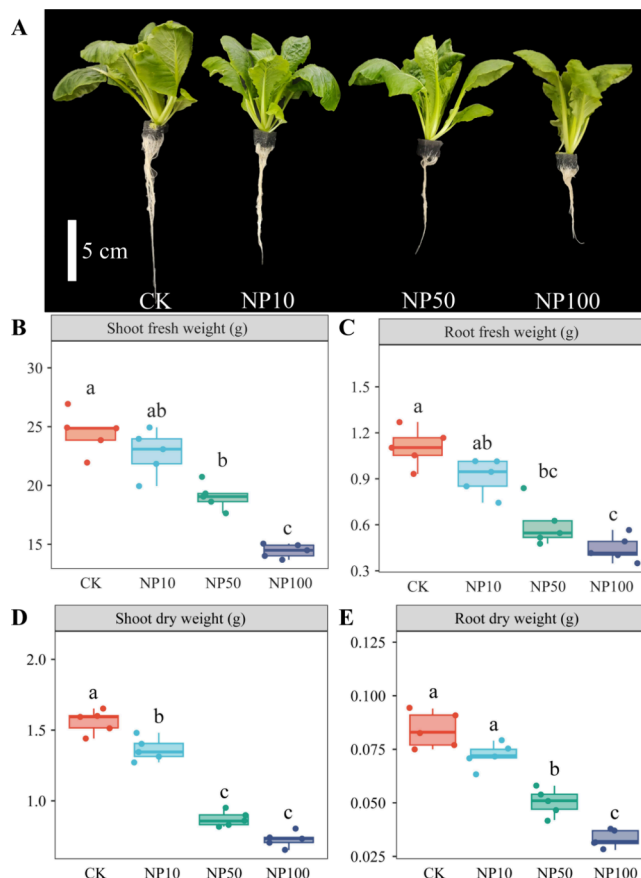


Figure 1. Effects of different concentrations of PS-NPs on pakchoi (A) growth phenotype, (B) shoot fresh weight, (C) root fresh weight, (D) shoot dry weight, and (E) root dry weight. Data are presented as mean ± SD ($n = 5$). Lowercase letters indicate statistically significant differences among treatments ($p < 0.05$).

deionized water, dried with absorbent paper, and cut off from the rhizome's and the stem's junction. An electronic balance (Mettler Toledo, XPR404S/AC) was used to accurately weigh the root and shoot of each pakchoi plant and recorded as fresh weight. Then, the samples were placed in the oven, dried at 60 °C, and the dry weight of shoots and roots.

2.4. CLSM Observation. Following exposure to fluorescent PS-NPs, pakchoi samples were gathered for the CLSM analysis to establish the potential accumulation of PS-NPs in both the roots and leaves. Each plant's root and leaf sections were separated and washed with distilled water to eliminate any surface PS-NPs. The root tips and leaves were cut out, placed on a glass slide filled with distilled water, and covered with a coverslip. The sectioned tissues were analyzed using a CLSM instrument (Leica TCS SP8, Leica Microsystems), and image acquisition was done using the software LAS X 3.5.6.21594 (Leica Microsystems). The excitation and emission wavelengths utilized for the analysis were 535 and 610 nm. The lens used provided a magnification of ×10, with the zoom factor adjusted to 0.75 to cover a larger sample region within the analysis area. The Z-step size was configured to 1 μm, scanning was performed in the XYZ direction,

and the scan speed was set at 400 Hz. Data was acquired using a HyD sensor in standard mode at a gain factor of 117.1%, and time gating was applied from 6.72 to 12 ns to reduce autofluorescence detection.

2.5. SEM Observation. In order to investigate the transport route of PS-NPs in pakchoi, seedlings were gathered and washed after being exposed to PS-NPs at varying concentrations. Subsequently, the roots and petioles were obtained for SEM analysis. The samples were immersed in a solution containing 2.5% glutaraldehyde at a pH of 7.4 for 2 h. They were then washed thrice with 0.1 M phosphate buffer (pH 7.2) and subsequently treated with 1% osmic acid at a temperature of 4 °C for another 2 h. Following this, the samples underwent dehydration through a graded ethanol series and were dried to a critical point. Finally, an approximately 1 nm-thick layer of gold was sputter-coated onto the samples for a duration of 30 s. Finally, the structure was observed with a GeminiSEM 300 scanning electron microscope.

2.6. RNA Extraction and Transcriptome Sequencing. In order to examine the impact of PS-NPs on transcription levels, we swiftly froze pakchoi leaves that had been exposed to varying concentrations of PS-NPs in liquid nitrogen. A Flying Shark Plant Total RNA Kit (Nobelab, Beijing, China) was used to extract total RNA. Nanodrop (Thermo Scientific, NC2000) was used to detect the purity of RNA. OD260/280 values of all RNA ranged from 2.203 to 2.294, and OD260/230 values ranged from 2.101 to 2.181, indicating that the purity of RNA met the requirements for library construction. Shanghai Peisenol Biotechnology Co., Ltd. accomplished transcriptome sequencing. Refer to our previous research for the specific steps.⁵⁰ Differential expression analysis between two comparison groups was performed using the DESeq software (version 1.20.0). DESeq was used to analyze differences in gene expression, with the following criteria for screening differentially expressed genes: an absolute log₂ fold change $|\log_2\text{FoldChange}| > 1$ and a significance threshold of *p* value < 0.05.

2.7. DAB and NBT Staining. To explore the effect of different concentrations of PS-NPs on the accumulation of hydrogen peroxide (H₂O₂) in pakchoi, the leaves of different treatments of pakchoi were cut and wholly immersed in 1 mg mL⁻¹ 3,3'-diaminobenzidine (DAB, pH 3.8), vacuumed, and maintained at negative pressure at -0.1 MPa for 30 min, stood at 25 °C for 12 h, and then decolorized in a water bath at 80 °C with 95% alcohol.

To test whether PS-NPs affect superoxide anion (O₂⁻) accumulation, the pakchoi leaves with different treatments were immediately placed in a brown bottle containing 1 mg mL⁻¹ nitro blue tetrazolium (NBT, pH 7.8) to submerge the leaves in the dyeing solution completely. Vacuum -0.1 MPa to maintain negative pressure for 30 min, then stand at room temperature and pressure for 60 min and pour off the NBT staining solution. Add 95% alcohol to the brown bottle, take a water bath at 80 °C, change the alcohol every 10 min, and take it out for photos after the green of the leaves has completely faded. DAB and NBT solutions were purchased from Coolaber Science & Technology; the product numbers are SL1805 and SL18061.

2.8. Detection of Malondialdehyde Content and Antioxidant Enzyme Activity. Malondialdehyde (MDA) content, superoxide dismutase (SOD), peroxidase (POD), catalase (CAT), glutathione POD (GPX) and glutathione-S-transferase (GST) activities were measured using kits purchased from Beijing Solebao Biotechnology Co., Ltd. The product numbers are BC0020, BC0170, BC0090, BC0200, BC1190, and BC0350.

2.9. Determination of Endogenous Auxin, Zeatin, and Abscisic Acid. The levels of endogenous auxin (IAA), zeatin (ZT), and abscisic acid (ABA) in pakchoi were analyzed using high-performance liquid chromatography (HPLC) to investigate the influence of various PS-NP concentrations on hormonal balance.

To configure the standard curve solution, first, 992 μL of methanol solution was added to a 1.5 mL centrifuge tube. Next, 2 μL of each hormone standard stock solution was incorporated at a concentration of 500 μg·mL⁻¹. It was thoroughly mixed to prepare a final working stock solution at a concentration of 1 μg mL⁻¹. Subsequently, ultrapure water was used to dilute the IAA, ZT, and ABA stock

solutions to concentrations of 0.1, 0.2, 0.5, 1, 2, 5, 10, 20, 50, 100, and 200 ng mL⁻¹, which were utilized for the preparation of the standard curve.

The pakchoi leaves were ground with liquid nitrogen until fully pulverized. An accurate measure of 0.1 g of the sample was then placed in a test tube. To this was added 10 mL of acetonitrile solution, alongside 8 μL of internal standard mother liquor. The mixture was extracted overnight at 4 °C. Then, a refrigerated centrifuge (Eppendorf, 5418R) was centrifuged at 4 °C for 12,000g for 5 min to collect the supernatant. For the remaining pellet, another 5 mL of an acetonitrile solution was used to extract it twice. The resulting supernatant was combined and purified with an appropriate amount of C18 and GCB packings to remove impurities. This mixture was again centrifuged at 12,000g for 5 min at 4 °C. The supernatant was collected, dried under a stream of nitrogen, and then reconstituted in 400 μL of methanol. Finally, the solution was filtered through a 0.22 μm organic phase filter membrane. Repeated measurements were taken five times per treatment, and the hormone content was calculated according to the standard curve. IAA, ZT, and ABA standards were purchased from Sigma.

2.10. Weighted Gene Coexpression Network Analysis (WGCNA). The WGCNA package in R was utilized for conducting a comprehensive coexpression analysis.⁵¹ The specific method of WGCNA is described in [Experiment S1](#).

2.11. qRT-PCR Analysis. The first strand of cDNA was synthesized from 1 μg of total RNA in a 20 μL reaction volume using Rescript II RT SuperMix reverse transcriptase (Nobelab). Quantitative real-time PCR (qRT-PCR) was performed in 96-well blocks on a CFX96 Touch Real-Time PCR System (Bio-Rad, Hercules, CA, USA) using a 2 × SYBR Premix UrTaqII (Nobelab) with a total reaction volume of 20 μL.⁵⁰ *BrActin* served as the housekeeping gene, and the 2^{-ΔΔCT} method was employed to determine the relative expression levels of the target gene. [Table S1](#) provides the sequences of the primers utilized for qRT-PCR.

2.12. Statistical Analyses. The statistical analysis was performed using SPSS version 22.0. To identify significant differences, we employed one-way ANOVA followed by Duncan's tests, with a *p* value of less than 0.05 indicating statistical significance. The outcomes were displayed as the mean plus or minus the standard deviation (SD), derived from at least three independent replicates. The graphs were prepared using Microsoft PowerPoint v.2016 and Adobe Photoshop CS6.

3. RESULTS

3.1. Effect of PS-NPs on Pakchoi Biomass. There were significant differences in the effects of PS-NPs at varying concentrations on the biomass of the pakchoi. Specifically, no significant difference in biomass was observed for pakchoi treated with 10 mg L⁻¹ PS-NPs compared to the CK ([Figure 1](#)). However, as the concentration of PS-NPs increased to 50 and 100 mg L⁻¹, a notable decline in biomass was recorded across all parts of pakchoi. The shoot fresh weight decreased by 22.17 and 41.09%, while the root fresh weight decreased by 45.58 and 59.71%. Similarly, the shoot dry weight exhibited reductions of 44.11 and 53.35%, and the root dry weight decreased by 40.00 and 60.48%, respectively ([Figure 1B–E](#)). The results indicate that if soil NP pollution is not effectively managed, it will persistently worsen, ultimately inhibiting crop growth.

3.2. Distribution of PS-NPs in Pakchoi. CLSM observations revealed that no red fluorescence was detected in the roots and leaves under CK treatment, indicating the absence of red autofluorescence in the pakchoi plant. However, red fluorescence was observed in the roots of pakchoi treated with varying concentrations of PS-NPs, with stronger red fluorescence intensity correlating with higher PS-NP concentrations ([Figure 2A](#)). SEM analysis showed that after entering

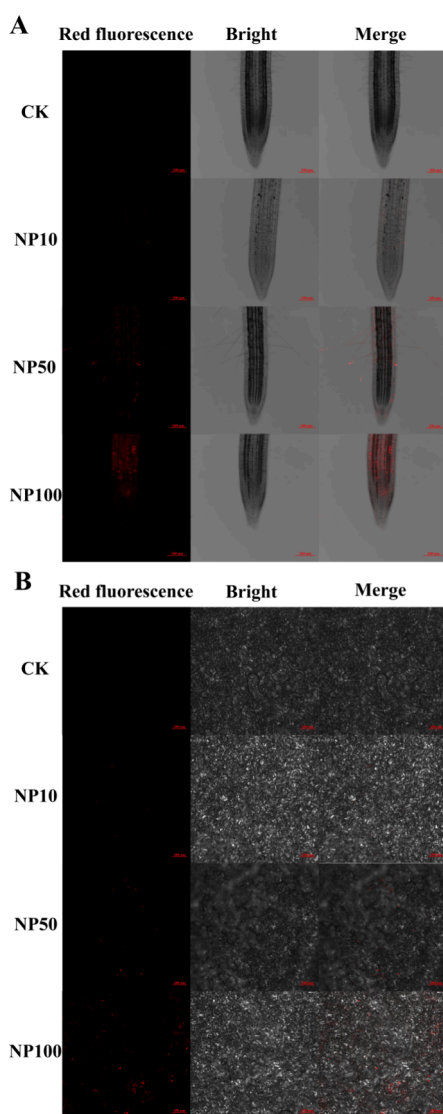


Figure 2. Utilizing CLSM, the impact of various concentrations of PS-NPs on the accumulation of PS-NPs in pakchoi (A) roots and (B) leaves was examined.

the roots, PS-NPs were primarily localized within the xylem vessels (Figure 3A–C). Subsequently, we found that PS-NPs were transported from the root xylem vessels to the xylem vessels of the petiole as they moved toward the shoot (Figure 3D–F). Ultimately, PS-NPs were transferred into the leaves via the xylem vessels of the petiole, resulting in the observation of varying intensities of red fluorescence in the leaves (Figure 2B).

3.3. Effect of PS-NPs on the Transcription Level of Pakchoi. As illustrated in Figure 4, PS-NPs significantly influence the transcriptional levels in pakchoi. Compared with the CK, NP10 treatment resulted in the inhibition of 626 genes and the activation of 716 genes (Figure S2A). Notably, as the concentration of PS-NPs increased, the effects on the transcriptional levels of pakchoi intensified. Specifically, under NP50 and NP100 treatments, the expressions of 831 and 1306 genes were significantly upregulated, while the expressions of 928 and 1259 genes were significantly downregulated (Figure S2B,C). The Venn diagram further revealed that a total of 602 common differentially expressed genes (DEGs) were identified across the various concen-

trations of PS-NPs (Figure S2D). Additionally, the results of the GO enrichment analysis indicated that the DEGs were predominantly enriched in the oxidoreductase activity term across different concentrations of PS-NP treatment (Figure S3).

3.4. Effect of PS-NPs on the Expression of Antioxidant Genes in Pakchoi. In comparison to the CK, the expression levels of antioxidant genes (*SOD*, *POD*, *CAT*, *GPX*, and *GST*) in pakchoi treated with PS-NPs at varying concentrations exhibited significant changes (Figure S4). Notably, the expression of the *BrSODs* gene was inhibited by PS-NPs, with the most pronounced inhibitory effect observed at a concentration of 100 mg L⁻¹. Conversely, the expressions of the *BrPOD17*, *BrCAT2*, and *BrGSTs* genes in pakchoi were significantly elevated following PS-NP treatment. The expression of *BrGPX7* showed a slight reduction at a concentration of 10 mg L⁻¹, increased dramatically at 50 mg L⁻¹, and was significantly inhibited at 100 mg L⁻¹.

3.5. Effect of PS-NPs on the Antioxidant System of Pakchoi. PS-NPs regulate the accumulation of ROS in pakchoi by modulating the antioxidant enzyme activity. This study found a positive correlation between the accumulation of H₂O₂, O₂⁻, and MDA in pakchoi and the concentration of PS-NPs. Specifically, higher concentrations of PS-NPs corresponded to increased levels of H₂O₂, O₂⁻, and MDA (Figure 4A–C). However, the activities of various antioxidant enzymes exhibited different trends in response to the PS-NP treatment. Compared to the CK, PS-NP treatment significantly inhibited SOD activity, with the most pronounced inhibition observed at a PS-NP concentration of 100 mg L⁻¹ (Figure 4D). In contrast, POD activity significantly increased with rising PS-NP concentrations (Figure 4E). No significant differences were observed in CAT and GST activities between NP10 and NP50 treatments; however, both enzyme activities were significantly elevated compared to those of CK. Under NP100 treatment, CAT and GST activities were significantly higher than those in other treatments (Figure 4F,H). Furthermore, GPX activity in pakchoi showed a significant increase under NP10 and NP50 treatments but decreased significantly under NP100 treatment (Figure 4G).

3.6. Effects of PS-NPs on Endogenous Hormone Content and Signal Transduction. Pakchoi responds to varying concentrations of PS-NP stress by regulating endogenous hormone homeostasis. Compared to the CK, treatments with NP10, NP50, and NP100 resulted in reduced levels of IAA and ZT, while the ABA content increased (Figure 5A–C). As the concentration of PS-NPs rises, the effects on the hormone content become more pronounced. At a PS-NP concentration of 100 mg L⁻¹, pakchoi exhibited decreases of 65.10 and 83.02% in IAA and ZT contents, respectively, alongside a 51.22% increase in ABA content (Figure 5A–C). Furthermore, PS-NPs influenced the expression of genes associated with IAA, cytokinin (CTK), and ABA signal transduction pathways (Figure 5D–F). In the IAA signal transduction pathway, the expressions of *AUX1*, *ARF*, *SAUR*, and *GH3* genes were inhibited, whereas the *AUX/IAA* expression was activated across different concentrations of PS-NP treatment (Figure 5D). Treatment with varying concentrations of PS-NPs also inhibited the expression of *CRE1*, *AHP*, and *A-ARR* genes within the CTK signal transduction pathway (Figure 5E). Additionally, PS-NP treatment activated *PYR/PYL* and *SnRK2* in the ABA signal

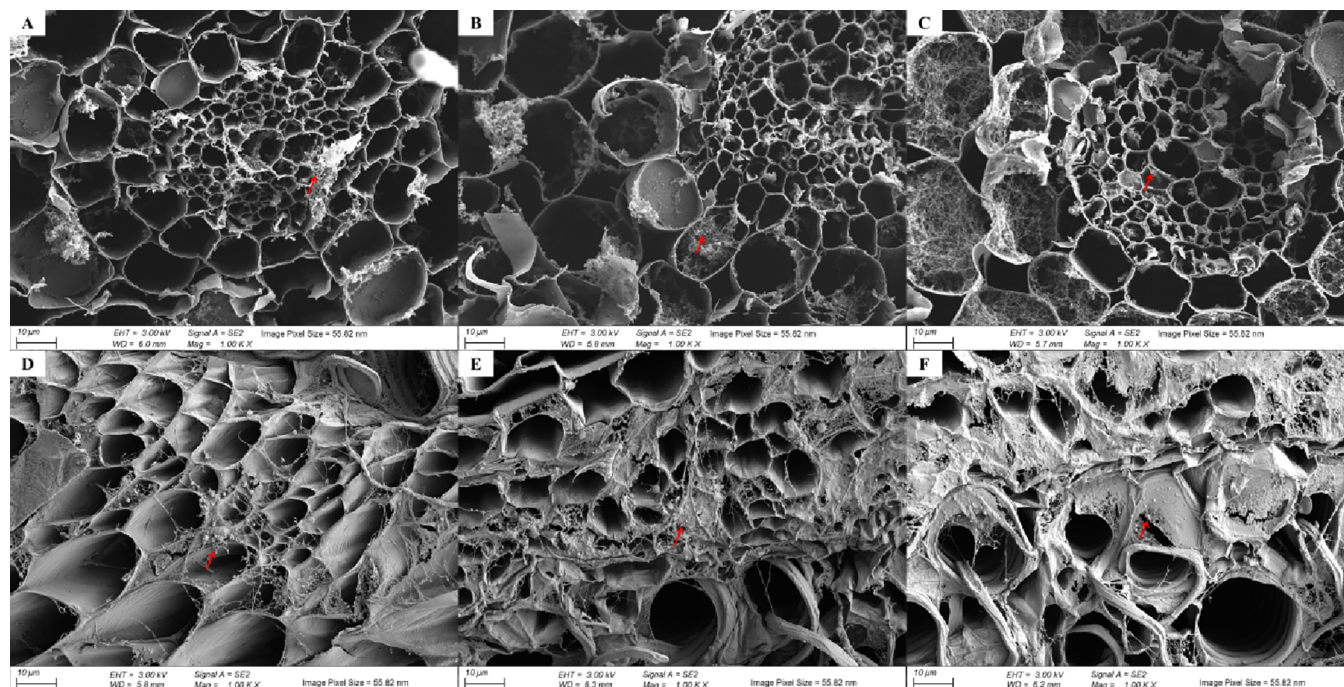


Figure 3. SEM was utilized to examine the dispersion of PS-NPs in the roots of pakchoi (A–C) and the petioles (D–F) after treatment with varying concentrations of PS-NPs.

transduction pathway while concurrently repressing the expression of *PP2Cs* (Figure 5F).

3.7. Effect of PS-NPs on Transcription Factor Expression in Pakchoi. This study found that varying concentrations of PS-NPs significantly influenced the expression of transcription factors in pakchoi. Notably, higher concentrations of PS-NPs corresponded to an increased number of affected transcription factor families and differentially expressed transcription factors. Compared to the CK, the expression levels of 25, 29, and 30 different transcription factor families were significantly altered under NP10, NP50, and NP100 treatments, respectively, with a total of 113, 157, and 245 differentially expressed transcription factors observed (Figure S5). Additionally, we identified transcription factors that exhibited significant differences in expression and consistent expression trends across different concentrations of PS-NP stress. These transcription factors predominantly belong to 10 families, including NAC, MYB, bHLH, WRKY, G2-like, C2H2, LBD, ERF, B3, and bZIP (Figure S6).

3.8. WGCNA Results. To investigate the regulatory relationships between genes under various treatments, we performed a WGCNA using transcriptome sequencing data from pakchoi leaves subjected to different treatments. This analysis identified 10 distinct WGCNA modules, which were represented by a range of colors, including magenta, green, pink, red, black, blue, purple, yellow, brown, and turquoise (Figure S7A). Notably, the characteristic genes of the turquoise module exhibited a significant positive correlation with IAA, ZT content, and SOD activity while showing a negative correlation with ABA, MDA content; and the activities of POD, CAT, and GST (Figure S7B). Furthermore, a comprehensive analysis of the genes within the yellow module through KEGG enrichment indicated that these genes were predominantly enriched with peroxisome and plant hormone signal transduction pathways (Figure S7C).

3.9. qRT-PCR Validation. As shown in Figure S8, the expression patterns of the eight randomly selected DEGs are almost consistent in the transcriptome sequencing and qRT-PCR results, proving the transcriptome results' reliability.

4. DISCUSSION

4.1. PS-NPs Inhibit the Growth of Pakchoi. Extensive studies have established that NP exposure concentration-dependently inhibits seed germination and plant growth, leading to significant biomass reduction.^{17,34,38,52} In this study, the fresh and dry weights of pakchoi roots and leaves were diminished under NP50 and NP100 treatments, with the inhibitory effect of NP100 being particularly pronounced (Figure 1). These findings indicate that NPs represent a significant factor contributing to the decline in agricultural productivity and pose a threat to food security. And as the concentration of NPs in the environment increases, the accumulation of NPs in plants is expected to rise correspondingly, leading to more severe harm to plant health. In addition, Conti et al. showed that common fruits and vegetables (such as apples, lettuce, and carrots) contain a large amount of MPs, which enter the human body through diet.⁴⁶ Therefore, reducing the emission of plastics into soil, especially farmland, is a key means to ensure sustainable development of agriculture and reduce the intake of NPs in the human body.

4.2. Absorption, Transport, and Accumulation of PS-NPs in Pakchoi. Plant roots play a crucial role in absorbing water and nutrients, serving as the primary pathway for environmental pollutants to enter the plant. NPs present in soil and water adhere to the root surface and can penetrate the root through fissures.⁹ Furthermore, NPs with smaller particle sizes may directly enter root cells via endocytosis, potentially leading to cytotoxic effects.¹⁴ In this study, CLSM was employed to examine the roots of pakchoi treated with red fluorescently labeled PS-NPs. A significant amount of red fluorescence was detected in the roots (Figure 2A). Subsequently, SEM was

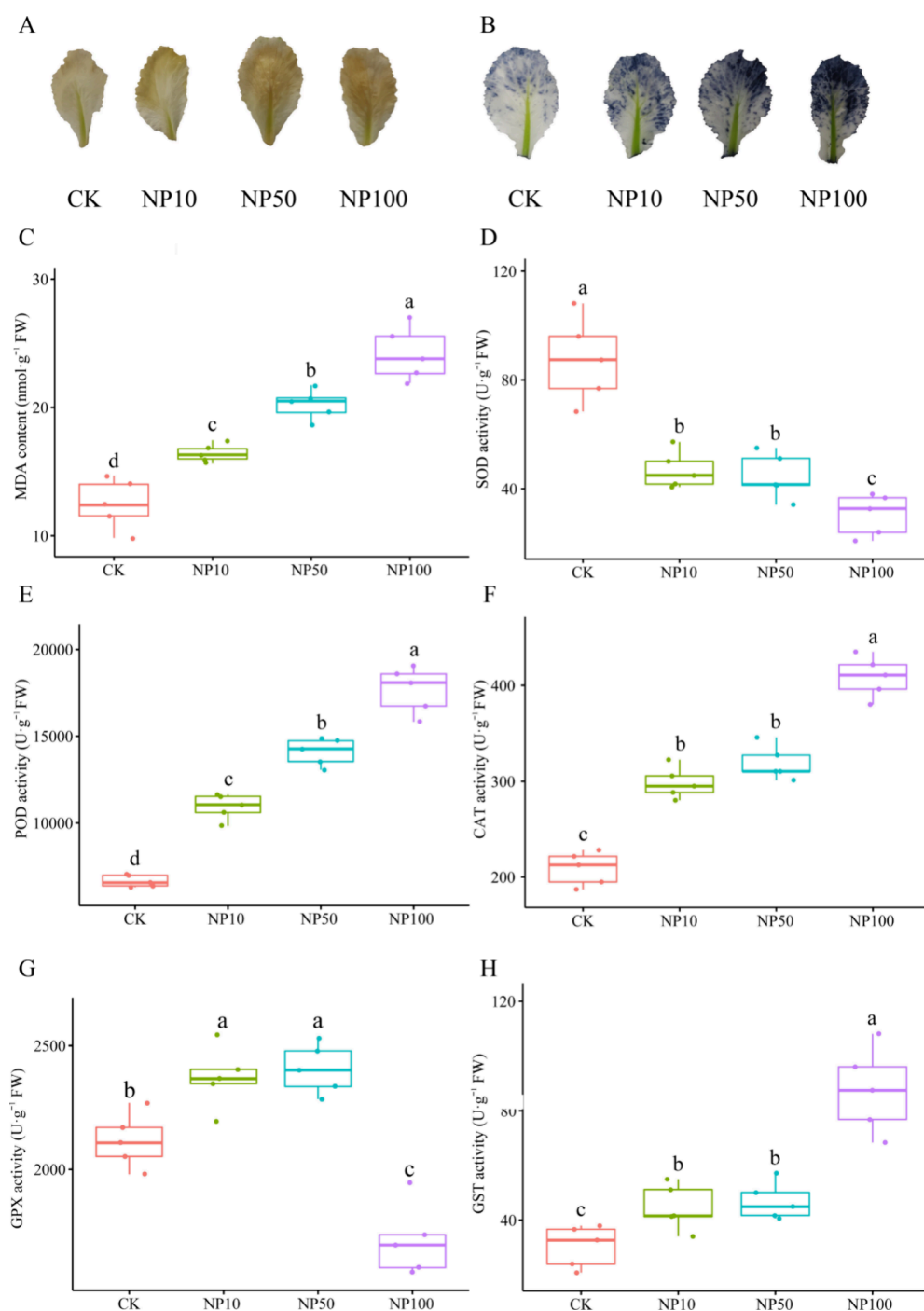


Figure 4. Effects of different concentrations of PS-NPs on pakchoi (A) hydrogen peroxide (H_2O_2), (B) superoxide anion (O_2^-), and (C) MDA accumulation and (D) SOD, (E) POD, (F) CAT, (G) GPX, and (H) GST activity. Data are presented as mean \pm SD ($n = 5$). Lowercase letters indicate statistically significant differences among treatments ($p < 0.05$).

utilized to analyze the root cross section, revealing that PS-NPs were distributed in the xylem vessels as aggregates (Figure 3A–C). This confirms the idea proposed by Li et al. that wheat and lettuce roots can absorb and transport MPs.⁹ Furthermore, studies have demonstrated that the roots of cucumber, cotton, corn, and rice are capable of absorbing and transporting NPs.^{33,34,53,54} The NPs absorbed by the roots enter the xylem vessels and are transported to the shoots with the help of a transpiration pull.⁹ Pakchoi has no stems, so we directly observed the distribution of NPs in petioles. Similar to the results in roots, NPs accumulated in the xylem vessels (Figure

3D–F). PS-NPs in xylem vessels are finally transported to the leaves with water and nutrients to observe red fluorescence in leaves treated with different PS-NPs (Figure 2B).

4.3. Oxidative Stress Induced by PS-NPs in Pakchoi.

This study demonstrated that exposure to varying concentrations of PS-NPs significantly increased the accumulation of H_2O_2 , O_2^- , and MDA in pakchoi leaves (Figure 4A–C), leading to oxidative damage and growth inhibition in pakchoi. However, the expression of different antioxidant genes and the activities of antioxidant enzymes exhibited distinct trends in response to PS-NP treatment at various concentrations.

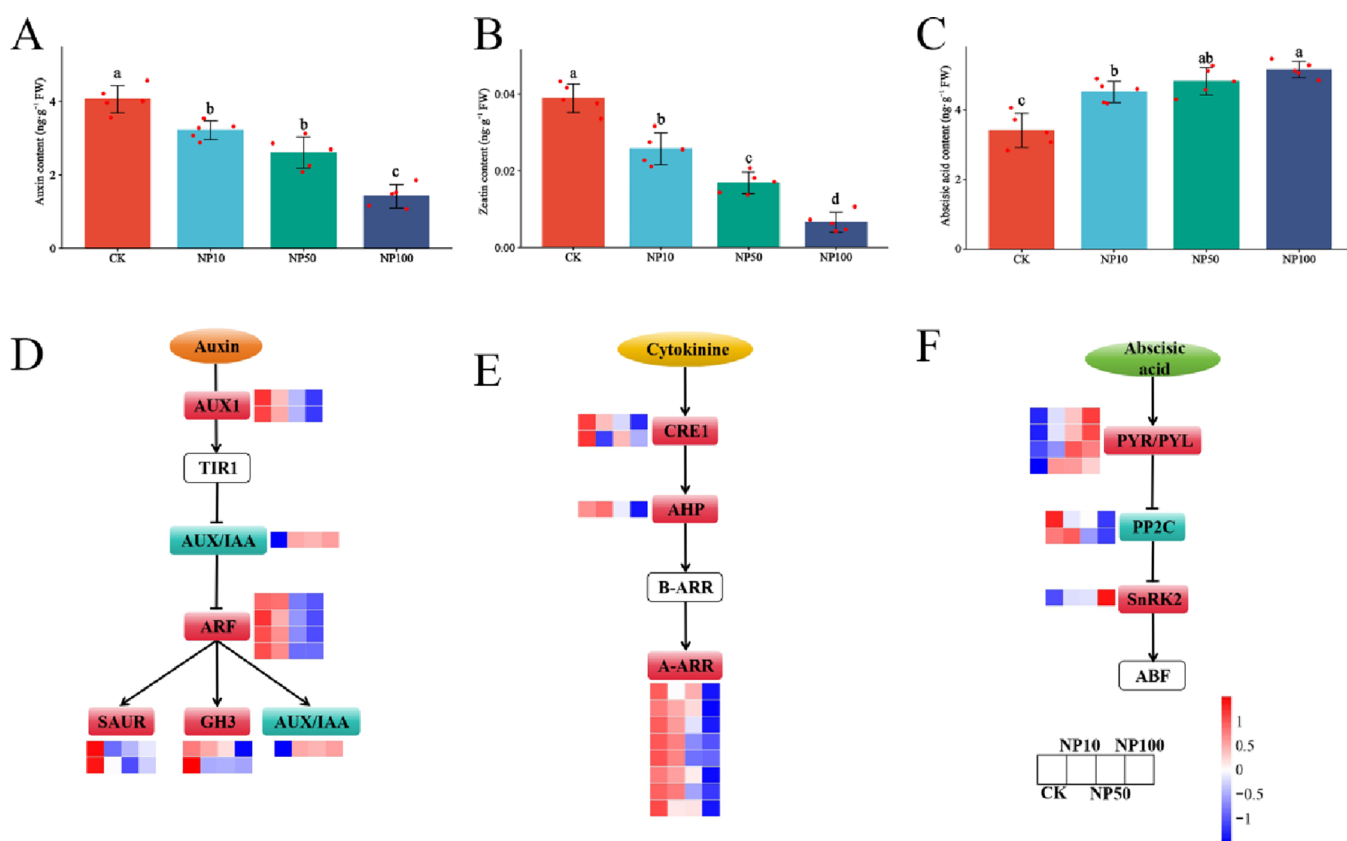


Figure 5. Effects of PS-NPs with different concentrations on endogenous hormone content and plant hormone signal transduction in pakchoi. Data are presented as mean \pm SD ($n = 5$). Lowercase letters indicate statistically significant differences among treatments ($p < 0.05$).

Notably, both the expressions of *BrSODs* and SOD activity were inhibited by PS-NPs, with the inhibitory effect intensifying as the concentration of PS-NPs increased (Figure S4 and Figure 4D). This may be because environmental stress that exceeds the tolerance threshold of organisms usually leads to a decrease in enzyme activity (such as SOD, POD, and CAT), which in turn induces ROS accumulation and cellular oxidative damage.^{39,54,55} The expression of *BrGPX7* and GPX activity was increased under NP10 and NP50 treatment but inhibited under NP100 treatment, supporting this view (Figures S4 and Figure 4G). At the same time, the expressions of *BrPOD17*, *BrCAT2*, and *BrGSTs* and the activities of POD, CAT, and GST were activated by PS-NPs to scavenge excess ROS (Figure S4 and Figure 4E,F,H) and alleviate the oxidative damage induced by PS-NPs.

To mitigate the oxidative damage caused by coercion, plants have developed various enzymatic systems to eliminate excessive ROS from their tissues, including SOD, POD, CAT, GPX, and GST. Among these, SOD catalyzes the conversion of O_2^- into H_2O_2 and O_2 , while POD, CAT, GPX, and GST are responsible for decomposing H_2O_2 into H_2O and O_2 .⁵⁶ In this study, we observed that SOD activity is diminished under NPS coercion, leading to a significant accumulation of O_2^- . H_2O_2 accumulates in significant quantities under NPs stress, leading to an increase in the activities of POD, CAT, GPX, and GST. However, at this stage, the pakchoi's intrinsic antioxidant enzyme system is insufficient to eliminate the excess H_2O_2 . Consequently, the accumulation of excess O_2^- and H_2O_2 results in severe oxidative damage to pakchoi.

4.4. PS-NPs Disrupt Endogenous Hormone Homeostasis and Interfere with Signal Transduction. Plant hormones serve as signaling molecules that regulate essential aspects of development, growth, and responses to environmental stress factors.⁵⁷ NPs influence growth and stress resistance by disrupting the homeostasis of plant endogenous hormones.^{21,22,58} Following exposure to PS-NPs, the ABA content in pakchoi leaves significantly increased, thereby enhancing the plant's resistance to PS-NPs (Figure 5C). Conversely, the levels of IAA and ZT were considerably reduced under PS-NP stress, which is a critical factor contributing to the inhibitory effects of PS-NPs on pakchoi growth (Figure 5A,B). Furthermore, NPs severely disrupt plant hormone signal transduction pathways.⁵⁹ In this study, PS-NPs inhibited the expression of the IAA transporter *AUX1* and positive regulatory factors such as *ARF*, *SAUR*, and *GH3* while increasing the expression of negative regulatory factors like *AUX/IAA*, thereby inhibiting IAA signal transduction (Figure 5D). Additionally, the expression of genes involved in the CTK signal transduction pathway, including *CRE1*, *AHP*, and *A-ARR*, was also suppressed by PS-NPs (Figure 5E). This inhibition may be attributed to the reduced levels of IAA and ZT in pakchoi under PS-NP treatment, further impeding its growth. In contrast, the ABA signaling pathway is activated due to the elevated endogenous ABA content (Figure 5F), which enhances pakchoi's tolerance to PS-NPs while inducing stomatal closure, inhibiting transpiration, and helping to restrict the transport of PS-NPs from roots to shoots.

4.5. Interaction of ROS and Plant Hormones under PS-NP Stress. Previous studies have reported the effects of NPs on plant ROS and hormones, but the interaction between

the two under NPs has not yet been elucidated.^{17,58} Previous studies have shown that H₂O₂ can oxidize IAA in plants, catalyze its degradation, and disrupt IAA homeostasis in plants.⁶⁰ In addition, POD, which relies on H₂O₂ production, also has auxin oxidase activity and can catalyze the oxidation reaction between IAA and oxygen molecules, thereby oxidizing IAA.⁶¹ In this study, under PS-NP treatment, H₂O₂ accumulation and POD activity in pakchoi leaves significantly increased, thereby oxidizing IAA and decreasing IAA content. As the concentration of PS-NPs increases, the H₂O₂ and POD activities also increase, resulting in lower and lower IAA content. There is also a close connection between the ABA signaling pathway and ROS. Overexpression of *PePYL4* enhanced poplar (*Populus tomentosa*) antioxidant enzyme activity and inhibited the accumulation of ROS.⁶² Under PS-NP treatment, the expression of *PYR/PYL* genes in pakchoi leaves significantly increased; enhanced POD, CAT, and GST activities; and accelerated the removal of ROS. Under salt and drought stress, overexpression of the *SnRK2* gene increased the antioxidant enzyme activity of transgenic plants and reduced ROS accumulation.^{63,64} In this study, PS-NPs increased the antioxidant enzyme activity by activating the expression of *SnRK2*, thereby promoting the removal of ROS.

4.6. Transcription Factors Regulate the Tolerance of Pakchoi to PS-NPs. Transcription factors play a crucial role in regulating plant growth, development, and stress adaptability. Previous studies have demonstrated that various transcription factors, including NAC, MYB, bHLH, WRKY, bZIP, G2-like, C2H2, LBD, ERF, and B3, are essential for plant responses to abiotic stress.^{65–75} However, there is currently a lack of research on transcription factors that regulate plant exposure to NP stress. In this study, we employed transcriptome sequencing to identify 38 transcription factors that exhibited significantly different expression levels and a consistent expression trend under varying concentrations of PS-NPs for the first time (Figure S6). These transcription factors may play a role in regulating the accumulation and tolerance of NPs in pakchoi. In future research, we plan to create mutants and overexpression lines for these transcription factors to further identify the critical factors that can inhibit NP accumulation and enhance resistance to NPs.

4.7. Shortcomings and Prospects of This Study. This study confirms that NPs can accumulate in pakchoi and negatively impact its growth. However, a limitation of this research is that the experiment was conducted under indoor hydroponic conditions, necessitating verification in real-field settings in future studies. Additionally, this investigation focused solely on the effects of PS-NPs on pakchoi. Future research should explore the transport and toxicity mechanisms of other types of NPs in crops and identify those NPs that are most harmful to crops for targeted prevention and control.

Reducing the production and emission of plastic products is the primary measure to control NP pollution; however, effective strategies are still required to address NP contamination. Previous studies have demonstrated that the exogenous application of selenium and brassinolide can effectively inhibit the accumulation of MPs in plants and mitigate their toxicity.^{76,55} These studies provide valuable ideas for mitigating NP pollution. Moving forward, our research will also concentrate on developing green and efficient methods to combat the escalating issue of NP pollution.

5. CONCLUSION

As a new pollutant, NP pollution continues to intensify due to the yearly increase in production and the low recycling rate. In this study, CLSM and SEM were used to find that the presence of NPs was observed in the roots, petioles, and leaves of pakchoi under PS-NP treatment, indicating that a large number of NPs will be ingested at the same time when humans eat pakchoi, which will pose a threat to human health. Moreover, the higher the concentration of PS-NPs used, the higher the accumulation of NPs in pakchoi, which means that if soil NP pollution is not controlled, more and more NPs will enter the human body through the diet. In this study, the effects of PS-NPs on pakchoi mainly include inducing the accumulation of ROS, leading to oxidative damage, destroying endogenous hormone homeostasis and signal transduction, and ultimately inhibiting growth. At the same time, pakchoi reduces the adverse effects of NPs through the interaction of ROS and hormones. In addition, this study screened 38 transcription factors that may be involved in regulating NP accumulation and tolerance, providing feasible ideas for plant resistance to NP breeding. This study confirmed that NPs can accumulate in vegetables, reducing agricultural productivity and posing significant challenges to food safety. Consequently, the primary focus for mitigating NP pollution should be the implementation of relevant policies aimed at reducing both the production and emissions of plastics. Furthermore, there is an urgent need to develop safe and effective methods to prevent the accumulation and toxicity of NPs in crops.

■ ASSOCIATED CONTENT

Supporting Information

The Supporting Information is available free of charge at <https://pubs.acs.org/doi/10.1021/acs.jafc.5c03590>.

Weighted gene coexpression network analysis (Experiment S1); primers used for quantitative real-time PCR (Table S1); TEM image and size distribution profile of PS-NPs (Figure S1); DEGs in pakchoi treated with PS-NPs at different concentrations (Figure S2); GO enrichment analysis of DEGs (Figure S3); effects of different concentrations of PS-NPs on the expression of antioxidant genes in pakchoi (Figure S4); expression of transcription factor families under different treatments (Figure S5); effects of different concentrations of PS-NPs on the expression patterns of different transcription factors in pakchoi (Figure S6); WGCNA for DEGs in pakchoi leaves and roots under CK, NP10, NP50, and NP100 treatment (Figure S7); validation of the expression of DEGs by qRT-PCR (Figure S8) (PDF)

■ AUTHOR INFORMATION

Corresponding Author

Peng Liu – College of Plant Protection, Shandong Agricultural University, Taian 271000, China; orcid.org/0000-0003-1833-495X; Email: liupeng2003@sdau.edu.cn

Authors

Zhiguo Liu – College of Plant Protection, Shandong Agricultural University, Taian 271000, China; College of Horticulture Science and Engineering, Shandong Agricultural University, Taian 271018, China

Mengzhan Qin – College of Plant Protection, Shandong Agricultural University, Taian 271000, China

Runze Li – College of Plant Protection, Shandong Agricultural University, Taian 271000, China

Willie J.G.M. Peijnenburg – Institute of Environmental Sciences, Leiden University, Leiden 2300 RA, The Netherlands; Center for the Safety of Substances and Products, National Institute of Public Health and the Environment, Bilthoven 3720 BA, The Netherlands; orcid.org/0000-0003-2958-9149

Long Yang – College of Plant Protection, Shandong Agricultural University, Taian 271000, China

Qinghua Shi – College of Horticulture Science and Engineering, Shandong Agricultural University, Taian 271018, China

Complete contact information is available at: <https://pubs.acs.org/10.1021/acs.jafc.5c03590>

Notes

The authors declare no competing financial interest.

ACKNOWLEDGMENTS

This work was financially supported by the foundation of Key Research and Development Program of Shandong Province, China (2022TZXD0025) and Modern Agricultural Technology Industry System of Shandong Province (SDAIT-25-07).

REFERENCES

- (1) Al-Salem, S. M.; Antelava, A.; Constantinou, A.; Manos, G.; Dutta, A. A review on thermal and catalytic pyrolysis of plastic solid waste (PSW). *J. Environ. Manage.* **2017**, *197*, 177–198.
- (2) Thompson, R. C.; Courteney-Jones, W.; Boucher, J.; Pahl, S.; Raubenheimer, K.; Koelmans, A. A. Twenty years of microplastic pollution research—what have we learned? *Science* **2024**, *386* (6720), No. eadl2746.
- (3) Pastor, B.; Agulló, V. Presence of microplastics in water and the potential impact on public health. *Rev. Esp. Salud Pública* **2019**, *93*, No. e201908064.
- (4) *Plastics-the Facts 2022*; PlasticsEurope. <https://plasticseurope.org/knowledge-hub/plastics-the-facts-2022/> (accessed 2025-03-15).
- (5) *Global Plastics Outlook: Plastics use in 2019*; OECD Environment Statistics (accessed 2025-03-15).
- (6) Wang, J.; Li, J.; Liu, S.; Li, H.; Chen, X.; Peng, C.; Zhang, P.; Liu, X. Distinct microplastic distributions in soils of different land-use types: a case study of Chinese farmlands. *Environ. Pollut.* **2021**, *269*, No. 116199.
- (7) Fuller, S.; Gautam, A. A procedure for measuring microplastics using pressurized fluid extraction. *Environ. Sci. Technol.* **2016**, *50* (11), 5774–5780.
- (8) Wang, L.; Wu, W. M.; Bolan, N. S.; Tsang, D. C.; Li, Y.; Qin, M.; Hou, D. Environmental fate, toxicity and risk management strategies of nanoplastics in the environment: Current status and future perspectives. *J. Hazard. Mater.* **2021**, *401*, No. 123415.
- (9) Li, L.; Luo, Y.; Li, R.; Zhou, Q.; Peijnenburg, W. J. G. M.; Yin, N.; Yang, J.; Tu, C.; Zhang, Y. Effective uptake of submicrometre plastics by crop plants via a crack-entry mode. *Nat. Sustainability* **2020**, *3* (11), 929–937.
- (10) Li, J.; Zhu, B.; Huang, B.; Ma, J.; Lu, C.; Chi, G.; Guo, W.; Chen, X. Vertical distribution and characteristics of soil microplastics under different land use patterns: A case study of Shouguang City, China. *Sci. Total Environ.* **2023**, *903*, No. 166154.
- (11) Luo, Y.; Li, L.; Feng, Y.; Li, R.; Yang, J.; Peijnenburg, W. J.; Tu, C. Quantitative tracing of uptake and transport of submicrometre plastics in crop plants using lanthanide chelates as a dual-functional tracer. *Nat. Nanotechnol.* **2022**, *17* (4), 424–431.
- (12) Sharma, V. K.; Ma, X.; Lichtfouse, E.; Robert, D. Nanoplastics are potentially more dangerous than microplastics. *Environ. Chem. Lett.* **2023**, *21*, 1933–1936.
- (13) Rist, S.; Baun, A.; Hartmann, N. B. Ingestion of micro-and nanoplastics in *Daphnia magna*—Quantification of body burdens and assessment of feeding rates and reproduction. *Environ. Pollut.* **2017**, *228*, 398–407.
- (14) Bandmann, V.; Müller, J. D.; Köhler, T.; Homann, U. Uptake of fluorescent nano beads into BY2-cells involves clathrin-dependent and clathrin-independent endocytosis. *FEBS Lett.* **2012**, *586* (20), 3626–3632.
- (15) Xu, L.; Liu, C.; Ren, Y.; Huang, Y.; Liu, Y.; Feng, S.; Zhong, X.; Fu, D.; Zhou, X.; Wang, J.; Liu, Y.; Yang, M. Nanoplastic toxicity induces metabolic shifts in *Populus× euramericana* cv. '74/76' revealed by multi-omics analysis. *J. Hazard. Mater.* **2024**, *470*, No. 134148.
- (16) Wang, Z.; Li, S.; Jian, S.; Ye, F.; Wang, T.; Gong, L.; Li, X. Low temperature tolerance is impaired by polystyrene nanoplastics accumulated in cells of barley (*Hordeum vulgare* L.) plants. *J. Hazard. Mater.* **2022**, *426*, No. 127826.
- (17) Sun, X. D.; Yuan, X. Z.; Jia, Y.; Feng, L. J.; Zhu, F. P.; Dong, S. S.; Liu, J.; Kong, X.; Tian, H.; Duan, J. L.; Ding, Z.; Wang, S. G.; Xing, B. Differentially charged nanoplastics demonstrate distinct accumulation in *Arabidopsis thaliana*. *Nat. Nanotechnol.* **2020**, *15* (9), 755–760.
- (18) Liu, Y.; Wei, L.; Yu, H.; Cao, X.; Peng, J.; Liu, H.; Qu, J. Negative impacts of nanoplastics on the purification function of submerged plants in constructed wetlands: responses of oxidative stress and metabolic processes. *Water Res.* **2022**, *227*, No. 119339.
- (19) Lian, J.; Wu, J.; Xiong, H.; Zeb, A.; Yang, T.; Su, X.; Su, L.; Liu, W. Impact of polystyrene nanoplastics (PSNPs) on seed germination and seedling growth of wheat (*Triticum aestivum* L.). *J. Hazard. Mater.* **2020**, *385*, No. 121620.
- (20) Tian, J.; Xu, Z.; Huang, W.; Han, D.; Dang, B.; Xu, J.; Jia, W. Physiobiochemical and transcriptional responses of tobacco plants (*Nicotiana tabacum* L.) to different doses of polystyrene nanoplastics. *Ind. Crop. Prod.* **2024**, *220*, No. 119218.
- (21) Arikan, B.; Alp, F. N.; Ozfidan-Konakci, C.; Yildiztugay, E.; Turan, M.; Cavusoglu, H. The impacts of nanoplastic toxicity on the accumulation, hormonal regulation and tolerance mechanisms in a potential hyperaccumulator-*Lemna minor* L. *J. Hazard. Mater.* **2022**, *440*, No. 129692.
- (22) Ozfidan-Konakci, C.; Yildiztugay, E.; Arikan, B.; Alp-Turgut, F. N.; Turan, M.; Cavusoglu, H.; Sakalak, H. Responses of individual and combined polystyrene and polymethyl methacrylate nanoplastics on hormonal content, fluorescence/photochemistry of chlorophylls and ROS scavenging capacity in *Lemna minor* under arsenic-induced oxidative stress. *Free Radical Biol. Med.* **2023**, *196*, 93–107.
- (23) Jiang, M.; Wang, B.; Ye, R.; Yu, N.; Xie, Z.; Hua, Y.; Zhou, R.; Tian, B.; Dai, S. Evidence and impacts of nanoplastic accumulation on crop grains. *Adv. Sci.* **2022**, *9* (33), No. 2202336.
- (24) Lian, J.; Liu, W.; Meng, L.; Wu, J.; Chao, L.; Zeb, A.; Sun, Y. Foliar-applied polystyrene nanoplastics (PSNPs) reduce the growth and nutritional quality of lettuce (*Lactuca sativa* L.). *Environ. Pollut.* **2021**, *280*, No. 116978.
- (25) Kik, K.; Bukowska, B.; Sicińska, P. Polystyrene nanoparticles: Sources, occurrence in the environment, distribution in tissues, accumulation and toxicity to various organisms. *Environ. Pollut.* **2020**, *262*, No. 114297.
- (26) De Felice, B.; Sugni, M.; Casati, L.; Parolini, M. Molecular, biochemical and behavioral responses of *Daphnia magna* under long-term exposure to polystyrene nanoplastics. *Environ. Int.* **2022**, *164*, No. 107264.
- (27) Huang, P.; Li, Z.; Liu, R.; Bartlam, M.; Wang, Y. Polystyrene nanoparticles induce biofilm formation in *Pseudomonas aeruginosa*. *J. Hazard. Mater.* **2024**, *469*, No. 133950.
- (28) Gao, X.; Xu, K.; Du, W.; Wang, S.; Jiang, M.; Wang, Y.; Han, Q.; Chen, M. Comparing the effects and mechanisms of exposure to polystyrene nanoplastics with different functional groups on the male reproductive system. *Sci. Total Environ.* **2024**, *922*, No. 171299.

- (29) Wu, Y.; Wang, J.; Zhao, T.; Sun, M.; Xu, M.; Che, S.; Pan, Z.; Wu, C.; Shen, L. Polystyrene nanoplastics lead to ferroptosis in the lungs. *J. Adv. Res.* **2024**, *56*, 31–41.
- (30) He, F.; Shi, H.; Guo, S.; Li, X.; Tan, X.; Liu, R. Molecular mechanisms of nano-sized polystyrene plastics induced cytotoxicity and immunotoxicity in *Eisenia fetida*. *J. Hazard. Mater.* **2024**, *465*, No. 133032.
- (31) Yu, Z.; Xu, X.; Guo, L.; Yuzuak, S.; Lu, Y. Physiological and biochemical effects of polystyrene micro/nano plastics on *Arabidopsis thaliana*. *J. Hazard. Mater.* **2024**, *469*, No. 133861.
- (32) Lian, J.; Liu, W.; Sun, Y.; Men, S.; Wu, J.; Zeb, A.; Yang, T.; Ma, L. Q.; Zhou, Q. Nanotoxicological effects and transcriptome mechanisms of wheat (*Triticum aestivum* L.) under stress of polystyrene nanoplastics. *J. Hazard. Mater.* **2022**, *423*, No. 127241.
- (33) Zhang, Y.; Yang, X.; Luo, Z. X.; Lai, J. L.; Li, C.; Luo, X. G. Effects of polystyrene nanoplastics (PSNPs) on the physiology and molecular metabolism of corn (*Zea mays* L.) seedlings. *Sci. Total Environ.* **2022**, *806*, No. 150895.
- (34) Zhou, C. Q.; Lu, C. H.; Mai, L.; Bao, L. J.; Liu, L. Y.; Zeng, E. Y. Response of rice (*Oryza sativa* L.) roots to nanoplastic treatment at seedling stage. *J. Hazard. Mater.* **2021**, *401*, No. 123412.
- (35) Jian, S.; Li, S.; Liu, F.; Liu, S.; Gong, L.; Jiang, Y.; Li, X. Elevated atmospheric CO₂ concentration changes the eco-physiological response of barley to polystyrene nanoplastics. *Chem. Eng. J.* **2023**, *457*, No. 141135.
- (36) Surgun-Acar, Y. Response of soybean (*Glycine max* L.) seedlings to polystyrene nanoplastics: Physiological, biochemical, and molecular perspectives. *Environ. Pollut.* **2022**, *314*, No. 120262.
- (37) Sun, H.; Bai, J.; Liu, R.; Zhao, Z.; Li, W.; Mao, H.; Zhou, L. Polyethylene microplastic and nano ZnO Co-exposure: Effects on peanut (*Arachis hypogaea* L.) growth and rhizosphere bacterial community. *J. Cleaner Prod.* **2024**, *445*, No. 141368.
- (38) Li, W.; Zhao, J.; Zhang, Z.; Ren, Z.; Li, X.; Zhang, R.; Ma, X. Uptake and effect of carboxyl-modified polystyrene microplastics on cotton plants. *J. Hazard. Mater.* **2024**, *466*, No. 133581.
- (39) Hua, Z.; Zhang, T.; Luo, J.; Bai, H.; Ma, S.; Qiang, H.; Guo, X. Internalization, physiological responses and molecular mechanisms of lettuce to polystyrene microplastics of different sizes: Validation of simulated soilless culture. *J. Hazard. Mater.* **2024**, *462*, No. 132710.
- (40) Huang, D.; Ding, L.; Wang, S.; Ding, R.; Qiu, X.; Li, J.; Hua, Z.; Liu, S.; Wu, R.; Liang, X.; Guo, X. Metabolomics reveals how spinach plants reprogram metabolites to cope with intense stress responses induced by photoaged polystyrene nanoplastics (PSNPs). *J. Hazard. Mater.* **2024**, *466*, No. 133605.
- (41) Zhang, H.; Liang, J.; Luo, Y.; Tang, N.; Li, X.; Zhu, Z.; Guo, J. Comparative effects of polystyrene nanoplastics with different surface charge on seedling establishment of Chinese cabbage (*Brassica rapa* L.). *Chemosphere* **2022**, *292*, No. 133403.
- (42) Lakshmikanthan, D.; Chandrasekaran, N. The Effect of humic acid and polystyrene fluorescence nanoplastics on *Solanum lycopersicum* environmental behavior and phytotoxicity. *Plants* **2022**, *11* (21), 3000.
- (43) Huang, D.; Shi, Z.; Shan, X.; Yang, S.; Zhang, Y.; Guo, X. Insights into growth-affecting effect of nanomaterials: Using metabolomics and transcriptomics to reveal the molecular mechanisms of cucumber leaves upon exposure to polystyrene nanoplastics (PSNPs). *Sci. Total Environ.* **2023**, *866*, No. 161247.
- (44) Giorgetti, L.; Spanò, C.; Muccifora, S.; Bottega, S.; Barbieri, F.; Bellani, L.; Castiglione, M. R. Exploring the interaction between polystyrene nanoplastics and *Allium cepa* during germination: Internalization in root cells, induction of toxicity and oxidative stress. *Plant Physiol. Biochem.* **2020**, *149*, 170–177.
- (45) Sun, C.; Yang, X.; Gu, Q.; Jiang, G.; Shen, L.; Zhou, J.; Li, L.; Chen, H.; Zhang, G.; Zhang, Y. Comprehensive analysis of nanoplastic effects on growth phenotype, nanoplastic accumulation, oxidative stress response, gene expression, and metabolite accumulation in multiple strawberry cultivars. *Sci. Total Environ.* **2023**, *897*, No. 165432.
- (46) Conti, G. O.; Ferrante, M.; Banni, M.; Favara, C.; Nicolosi, I.; Cristaldi, A.; Fiore, M.; Zuccarello, P. Micro-and nano-plastics in edible fruit and vegetables. The first diet risks assessment for the general population. *Environ. Res.* **2020**, *187*, No. 109677.
- (47) Liu, Z.; Qin, M.; Li, R.; Zhou, Y.; Yan, J.; Ahmad, P.; El-Sheikh, M. A.; Yang, L.; Liu, P.; Shi, Q. Transcriptional, physiological and ultrastructure levels revealed silicon enhanced cadmium detoxification and functional compound accumulation in pakchoi. *LWT-Food Sci. Technol.* **2025**, *215*, No. 117253.
- (48) Yu, Y.; Li, J.; Song, Y.; Zhang, Z.; Yu, S.; Xu, M.; Zhao, Y. Stimulation versus inhibition: The effect of microplastics on pak choi growth. *Appl. Soil Ecol.* **2022**, *177*, No. 104505.
- (49) Xie, Z.; Men, C.; Yuan, X.; Miao, S.; Sun, Q.; Hu, J.; Zhang, Y.; Liu, Y.; Zuo, J. Naturally aged polylactic acid microplastics stunted pakchoi (*Brassica rapa* subsp. *chinensis*) growth with cadmium in soil. *J. Hazard. Mater.* **2023**, *460*, No. 132318.
- (50) Liu, Z.; Wu, X.; Hou, L.; Ji, S.; Zhang, Y.; Fan, W.; Li, T.; Zhang, L.; Liu, P.; Yang, L. Effects of cadmium on transcription, physiology, and ultrastructure of two tobacco cultivars. *Sci. Total Environ.* **2023**, *869*, No. 161751.
- (51) Langfelder, P.; Horvath, S. WGCNA: an R package for weighted correlation network analysis. *BMC Bioinf.* **2008**, *9*, S59.
- (52) Guo, M.; Zhao, F.; Tian, L.; Ni, K.; Lu, Y.; Borah, P. Effects of polystyrene microplastics on the seed germination of herbaceous ornamental plants. *Sci. Total Environ.* **2022**, *809*, No. 151100.
- (53) Wang, Y.; Bai, J. J.; Wei, Y. J.; Zhao, C. X.; Shao, Z.; Chen, M. L.; Wang, J. H. Tracking and imaging nano-plastics in fresh plant using cryogenic laser ablation inductively coupled plasma mass spectrometry. *J. Hazard. Mater.* **2024**, *465*, No. 133029.
- (54) Li, X.; Zeng, G.; Du, X.; Zhou, R.; Lian, J.; Liu, J.; Guo, X.; Tang, Z. Effects of polyethylene and biodegradable microplastics on the physiology and metabolic profiles of dandelion. *Environ. Pollut.* **2024**, *352*, No. 124116.
- (55) Zhang, D.; Zhang, L.; Yuan, C.; Zhai, K.; Xia, W.; Duan, Y.; Zhao, B.; Chu, J.; Yao, X. Brassinolide as potential rescue agent for *Pinellia ternata* grown under microplastic condition: Insights into their modulatory role on photosynthesis, redox homeostasis, and AsA-GSH cycling. *J. Hazard. Mater.* **2024**, *470*, No. 134116.
- (56) Rajput, V. D.; Harish; Singh, R. K.; Verma, K. K.; Sharma, L.; Quiroz-Figueroa, F. R.; Meena, N.; Gour, V. S.; Minkina, T.; Sushkova, S.; Mandzhieva, S. Recent developments in enzymatic antioxidant defence mechanism in plants with special reference to abiotic stress. *Biology* **2021**, *10* (4), 267.
- (57) Waadt, R.; Seller, C. A.; Hsu, P. K.; Takahashi, Y.; Munemasa, S.; Schroeder, J. I. Plant hormone regulation of abiotic stress responses. *Nat. Rev. Mol. Cell Biol.* **2022**, *23* (10), 680–694.
- (58) Li, G.; Qiu, C.; Zhang, D.; Lv, M.; Liao, X.; Li, Q.; Wang, L. Effects of polystyrene nanoplastics (PSNPs) on the physiology of *Allium sativum* L.: Photosynthetic pigments, antioxidant enzymes, phytohormones, and nutritional quality. *Environ. Exp. Bot.* **2024**, *219*, No. 105654.
- (59) Li, Q.; Zhang, B.; Liu, W.; Zou, H. Strigolactones alleviate the toxicity of polystyrene nanoplastics (PS-NPs) in maize (*Zea mays* L.). *Sci. Total Environ.* **2024**, *918*, No. 170626.
- (60) Gazarian, I. G.; Lagrimini, L. M.; Mellon, F. A.; Naldrett, M. J.; Ashby, G. A.; Thorneley, R. N. Identification of skatolyl hydroperoxide and its role in the peroxidase-catalysed oxidation of indol-3-yl acetic acid. *Biochem. J.* **1998**, *333* (1), 223–232.
- (61) Savitsky, P. A.; Gazaryan, I. G.; Tishkov, V. I.; Lagrimini, L. M.; Ruzgas, T.; Gorton, L. Oxidation of indole-3-acetic acid by dioxygen catalysed by plant peroxidases: specificity for the enzyme structure. *Biochem. J.* **1999**, *340* (3), 579–583.
- (62) Li, Q.; Shen, C.; Zhang, Y.; Zhou, Y.; Niu, M.; Wang, H. L.; Lian, C.; Tian, Q.; Mao, W.; Wang, X.; Liu, C.; Yin, W.; Xia, X. *PePYL4* enhances drought tolerance by modulating water-use efficiency and ROS scavenging in *Populus*. *Tree Physiol.* **2023**, *43* (1), 102–117.
- (63) Zhang, Y.; Wan, S.; Liu, X.; He, J.; Cheng, L.; Duan, M.; Liu, H.; Wang, W.; Yu, Y. Overexpression of *CsSnRK2.5* increases

tolerance to drought stress in transgenic *Arabidopsis*. *Plant Physiol. Biochem.* **2020**, *150*, 162–170.

(64) Shao, Y.; Zhang, X.; van Nocker, S.; Gong, X.; Ma, F. Overexpression of a protein kinase gene *MpSnRK2.10* from *Malus prunifolia* confers tolerance to drought stress in transgenic *Arabidopsis thaliana* and apple. *Gene* **2019**, *692*, 26–34.

(65) Sun, L.; Zhang, P.; Li, W.; Li, R.; Ju, Q.; Tran, L. S. P.; Xu, J. The bifunctional transcription factor NAC32 modulates nickel toxicity responses through repression of root-nickel compartmentalization and activation of auxin biosynthesis. *J. Hazard. Mater.* **2024**, *480*, No. 135925.

(66) Zhu, N.; Duan, B.; Zheng, H.; Mu, R.; Zhao, Y.; Ke, L.; Sun, Y. An R2R3MYB gene *GhMYB3* functions in drought stress by negatively regulating stomata movement and ROS accumulation. *Plant Physiol. Biochem.* **2023**, *197*, No. 107648.

(67) Qiao, Q.; Huang, Y.; Dong, H.; Xing, C.; Han, C.; Lin, L.; Wang, X.; Su, Z.; Qi, K.; Xie, Z.; Huang, X.; Zhang, S. The PbbHLH62/PbVHA-B1 module confers salt tolerance through modulating intracellular Na⁺/K⁺ homeostasis and reactive oxygen species removal in pear. *Plant Physiol. Biochem.* **2024**, *210*, No. 108663.

(68) Yu, Y.; He, L.; Wu, Y. Wheat WRKY transcription factor TaWRKY24 confers drought and salt tolerance in transgenic plants. *Plant Physiol. Biochem.* **2023**, *205*, No. 108137.

(69) Mahiwal, S.; Pahuja, S.; Pandey, G. K. Structural-functional relationship of WRKY transcription factors: Unfolding the role of WRKY in plants. *Int. J. Biol. Macromol.* **2024**, *257*, No. 128769.

(70) Rahman, S.; Rehman, A.; Waqas, M.; Mubarik, M. S.; Alwutayd, K.; AbdElgawad, H.; Jalal, A.; Azeem, F.; Rizwan, M. Genome-wide exploration of bZIP transcription factors and their contribution to alkali stress response in *Helianthus annuus*. *Plant Stress* **2023**, *10*, No. 100204.

(71) Nagatoshi, Y.; Mitsuda, N.; Hayashi, M.; Inoue, S. I.; Okuma, E.; Kubo, A.; Murata, Y.; Seo, M.; Saji, H.; Kinoshita, T.; Ohme-Takagi, M. GOLDEN 2-LIKE transcription factors for chloroplast development affect ozone tolerance through the regulation of stomatal movement. *Proc. Natl. Acad. Sci. U. S. A.* **2016**, *113* (15), 4218–4223.

(72) Feng, Q.; Zhao, L.; Jiang, S.; Qiu, Y.; Zhai, T.; Yu, S.; Yang, W.; Zhang, S. The C2H2 family protein ZAT17 engages in the cadmium stress response by interacting with PRL1 in *Arabidopsis*. *J. Hazard. Mater.* **2024**, *465*, No. 133528.

(73) Gupta, K.; Gupta, S. Molecular and in silico characterization of tomato LBD transcription factors reveals their role in fruit development and stress responses. *Plant Gene* **2021**, *27*, No. 100309.

(74) Khoudi, H. SHINE clade of ERF transcription factors: A significant player in abiotic and biotic stress tolerance in plants. *Plant Physiol. Biochem.* **2023**, *195*, 77–88.

(75) Gao, J.; Ma, G.; Chen, J.; Gichovi, B.; Cao, L.; Liu, Z.; Chen, L. The B3 gene family in *Medicago truncatula*: Genome-wide identification and the response to salt stress. *Plant Physiol. Biochem.* **2024**, *206*, No. 108260.

(76) Tong, M.; Zhai, K.; Duan, Y.; Xia, W.; Zhao, B.; Zhang, L.; Chu, J.; Yao, X. Selenium alleviates the adverse effects of microplastics on kale by regulating photosynthesis, redox homeostasis, secondary metabolism and hormones. *Food Chem.* **2024**, *450*, No. 139349.